Surface Properties of Alkylsilane Treated Date Palm Fiber

Helanka Perera (hperera@hct.ac.ae)
Abu Dhabi Women's Campus, Higher Colleges of Technology
Anjali Goyal
Khalifa University of Science and Technology
Saeed Alhassan
Khalifa University of Science and Technology

Research Article

Keywords: Biodegradable, Silane coupling agents, Scanning electron microscopy, Thermal gravimetric analysis, Cellulose, Hydrophobicity

Posted Date: March 11th, 2022

DOI: https://doi.org/10.21203/rs.3.rs-1403599/v1

Abstract

The present work focuses on investigating the effect of *short chain alkylsilane* treatment on the surface characteristic of date palm (*Phoenix dactylifera*) fiber. Raw date palm fiber was treated with octylsilane and surface properties of treated fiber was investigated using thermogravimetric analysis (TGA), fourier transform infrared (FTIR) spectroscopy, scanning electron microscopy (SEM), contact angle analysis and X-ray diffraction (XRD) on configuring the thermal stability, chemical structures and surface properties (morphology, hydrophobicity and crystallinity). Thermal properties, hydrophobicity and crystallinity increased with introducing octylsilane compared to raw date palm fiber. The SEM and XRD experimental results showed that the alkylsilane treatment can effectively remove non-crystalline cellulosic materials. Thermal stability, hydrophobicity and crystallinity of the fibers were found to increase on alkylsilane-treatment. The results indicated that alkylsilane-treated DPFs were a suitable reinforcing substitute for hydrophobic polymer composite.

Introduction

Over the past decades, polymer composites incorporated natural renewable fiber materials have taken the attention of researchers due to their lightweight (which makes composites lighter), low cost, bio-renewable character, biodegradable and resistant to deforestation [1]. Many studies have demonstrated, conventional synthetic fibres has been replaced by natural fibres as reinforcing material on polymer composites [2–5].

The polymer composite matrix has a significant impact on the composite performance. The main component of the matrix of the polymer composite is reinforcing material. Due to the hydrophilicity of natural fibers, several downsides were discovered when natural fiber was used as a reinforcing material instead of synthetic fiber. The primary three main fiber components are cellulose, hemicellulose and lignin. These components are responsible for the hydrophilicity of the natural fibers, that impact incompatibility with hydrophobic polymers, i. e. a tendency to clump during processing and poor moisture resistance. Chemical treatment of the fiber surface is required to minimize the hydrophilic character of the natural fiber and promote adhesion. [6] According to the literature, numerous ways have been investigated for surface modification of fibers [7–9], with silane treatment being one of the more effective chemical methods for introducing surface hydrophobicity. [10–12]

In Gulf countries, the date palm is one of the most widespread plants among all other trees. The United Arab Emirates (UAE) is home to the most date palms of any country globally. It is said to have 40 million date palm trees and at least 200 cultivars, 68 of which are commercially valuable [13]. The UAE has 16,342,190 productive date palms in 2006, which produced 757,600 tons of dates [14]. The United Arab Emirates was just named the world's leading date palm cultivator, with 42 million trees, as revealed on March 15, 2009. Due to the more considerable amount of date palm production, a significant amount of waste is generated annually and burned directly in an open field, which causes damage to the environment and humans. Considering all problems caused by waste material can be used as renewable

materials on economically value product synthesis, such as crates, basketry, rope and furniture. Last decade, date palm fiber (DPF) as a reinforcing agent on polymer composite is one of the interesting topics in research.[9, 15]

In this study, *DPFs were chemically treated in the presence of short-chain alkyl silane to create a hydrophobic surface to assess their feasibility as a polymer composite reinforcing material*. Fourier transform infrared spectroscopy (FTIR), scanning electron microscope (SEM), thermal gravimetric analysis (TGA), contact angle and X-ray diffraction (XRD) analysis were used to investigate the chemical structure, morphology and physical properties (thermal, hydrophobicity and crystallinity) of raw and treated DPFs. This study aims to provide a systematic overview of how short-chain alkylsilane can be used to alter the surface and thermal properties of DPF.

Experimental Section

Materials

Octyltrichlorosilane (C8) was obtained from SigmaAldrich (St. Louis, MO, USA). Hexane was from Pharmco-Aaper (Brookfield, CT, USA). All chemicals were used as received. The raw date palm fiber (*Phoenix dactylifera*) meshes were collected from the Abu Dhabi Campus from Abu Dhabi, UAE (Fig. 1A). Date palm meshes were removed from the stem and sealed in polyethylene bags until the experiments were conducted (Fig. 1B). These DPF meshes were manually separated into single fibers and washed with distilled water to remove dust particles, sand and impurities. Cleaned fibers were dry for 24 hours at room temperature.

Methods

Preparation of the treated date palm fibers

DPF (1 g) was cleaned and reacted with 1 g of C8 in glass vials with 250 mL of hexane to cover the DPF completely. The silane reaction was carried out in a shaker for 4 hours at 50°C and 200 rpm. After shaking, treated DPFs were rinsed three times with 100 mL hexane to remove the unreacted C8 coupling agent. After that, the materials were maintained at room temperature until the characterizations were performed.

Measurements and characterization

Thermo-gravimetric analysis (TGA)

TGA was performed to identify the degradation characteristics of the C8 treated fiber with the raw DPF. Hereafter, the grafted amount of C8 on the treated DPF was quantified using a TA Instruments, Model SDT 650 Thermogravimetric Analyzer (TA Instruments, New Castle, DE, USA). The treated DPF and raw DPF samples were heated from 20 to 900°C with a heating rate of 20°C/min in high purity nitrogen gas.

Fourier transform infrared (FTIR) spectroscopy

FTIR spectra were taken using a Perkin Elmer Frontier FTIR spectrometer (PerkinElmer Genetics Inc., Waltham, MA, USA). The scanning range was from 600 to 4000 cm^{-1} with a spectral resolution of 4 cm^{-1} and 32 scans.

Scanning electron microscopy (SEM)

The surface morphology was carried out by scanning electron microscopy (SEM) using FEG Quanta 250 (FEI Company, Hillsboro, OR, USA) instrument of the raw and C8 treated DPFs under high vacuum mode operated at an acceleration voltage of 5 kV a working distance of about 10 mm. For SEM studies, each sample was attached to double-sided carbon adhesive tape on the top of an aluminum stud. The samples were then made conductive by the sputtering of Au/Pd.

Contact angle analysis

For contact angle measurements, the raw and C8 treated DPF samples were prepared on a glass slide by placing fibers close to each other with the help of double-sided sticky tape, as shown in Fig. 2. Water contact angle measurements were then performed using the static drop method at room temperature using KRÜSS DSA25 Series (KRÜSS Scientific Instruments, Inc., Matthews, NC, USA). Deionized water was used as a probe liquid (0.3 µl dispense volume) at a frequency of 20 in a time interval of 3000 milliseconds. Ten images from different locations on the surface were taken for each sample, with the average reported for the contact angle.

X-ray diffraction (XRD)

Diffraction (XRD) patterns were collected using X'Pert PRO powder diffractometer (Cu-Ka radiation 1.5406 Å, 45 kV, 40mA) in the range of 5–80°, 2θ scale. The empirical method was used to obtain the crystallinity index (CI) of the samples [16], as shown in Eq. (1):

$$CI = \left(\frac{I_{cr} - I_{am}}{I_{cr}} \right) * 100 (1)$$

where I_{cr}, and I_{am} represent the crystalline intensity and amorphous intensity at an angle (2θ). I_{cr} is the crystalline peak corresponding to the intensity of approximately 23° and I_{am} is the amorphous peak corresponding to the intensity of approximately 19°.

Results And Discussion

Thermogravimetric analysis (TGA)

The TGA thermograms for raw and C8 treated DPF samples are shown in Fig. 3. To more clearly show the nature of thermal degradation, the first derivative of mass losses are potted against temperature. Figure 3(A), the derivative curves of raw DPF and C8 treated DPF, showed three major mass losses in the temperature range of 25–400 ^{O}C. The first mass loss was associated with the removal of physically adsorbed water. The other two major degradations occur between 200–400 ^{O}C, which is related to the degradation of hemicellulose and lignin. [17, 18] After modification of C8 on DPF, a decrease in mass losses of hemicellulose and lignin were observed on the C8-DPF compared to raw DPF. It indicates C8 silane treatment can remove hemicellulose and lignin or non-crystalline cellulose present in the fiber. [19] A significant broad mass loss occurred between 375–750 ^{O}C in raw and C8 treated DPF, as shown in Fig. 3(B). For raw DPF, this broad mass loss was attributed to the degradation of cellulosic and other non-cellulosic material present in the DPF. [17, 18] The decomposition of C8-DPF gave a well-resolved peak around 520 ^{O}C, in addition to the broad mass loss, as shown in Fig. 3(B). According to the literature, the pronounced mass loss in the temperature range 450–600 ^{O}C was attributed to the decomposition of the hydrocarbon chain of C8. [20] TGA thermograms confirm raw DPFs were successfully modified with the C8 silane coupling agent.

Fourier transform infrared (FTIR) spectroscopy

The structural changes in the fiber surface before and after treatment were investigated using FTIR spectroscopy to establish the chemical efficiency of silane treatments. FTIR spectra of the raw and C8-DPF are shown in Fig. 4. The common peak positions for raw and C8-DPF are indicated with the dotted line. The broad peak ranging from 3660 cm^{-1} to 2990 cm^{-1} was because of hydroxyl groups stretching vibration present in cellulose, hemicellulose, and lignin. The vibration peaks at 2919 cm^{-1} and 2854 cm^{-1} revealed asymmetric and symmetric CH_2 stretching in cellulose/hemicellulose, respectively. The peaks at 1730 cm^{-1}, 1620 cm^{-1}, 1245 cm^{-1} and 1023 cm^{-1} are corresponded to ester carbonyl group stretching, C = O stretching in carboxylic acid in hemicellulose, O-CH_3 stretching in lignin and C-O stretching vibration, respectively, for both raw and C8-DPF. [9, 15, 21] After C8 silane treatment, new absorption bands are appeared in the region, between 1200 to 500 cm^{-1}, which are specific for silane coupling agents. Indeed, two new bands emerge at 1100 cm^{-1} and 670 cm^{-1}, which are caused mainly by the vibration of Si-O-cellulose and Si-O-Si on the fiber is shown in Fig. 4 shows the * symbol. [9, 22, 23] Consequently, the proposed procedure has been demonstrated to be effective in fabricating chemically treated DPF surfaces with C8 silane coupling agents.

Scanning electron microscopy (SEM)

SEM is a powerful tool for studying the surface morphology of fibers. Figure 5 shows the relevant SEM images of the raw and C8 modified DPF. Figures 5(A) and (B) show the SEM images of the longitudinal surface of raw and C8-DPF. DPF has a cylindrical shape both with and without treatment, as shown in Figs. 5(A) and (B). Silane treatment did not damage the shape of the fiber. When comparing raw DPF to C8 treated fiber, the diameter of the silane treated fiber is smaller. The removal of hemicellulose and lignin

from the fibers causes the diameter to shrink. The findings are consistent with recent experimental data on oil palm fiber by Yousif et al. [24], kenaf fiber by Chin and Yousif et al. [25] and hemp fiber by Sawpan et al. [26]. As illustrated in Figs. 5(A) and 5(B), the raw DPF surface seems rougher, whereas C8-DPF appears to develop a smoother surface due to the filling up of the spaces by silane treatment. Figures 5(C) and (D) show SEM micrographs of raw and C8-DPF in the cross sections, respectively. With C8 treatment, fiber pores are increased due to the removal of hemicellulose and lignin.

Contact angle analysis

Hydrophobicity of the surface was measured using contact angle measurements. Water contact angles of raw and C8 treated DPF are shown in Fig. 6. The raw DPF had a contact angle of 66.8 ^{O}. Free hydroxyl groups present on hemicellulose and lignin makes raw DPF hydrophilic. [27] The hydrophobicity of the raw DPF was enhanced to 116 ^{O} with modification of the DPF with the C8 silane coupling agent. Introducing low surface energy material improved the hydrophobicity of the material. [28]

X-ray diffraction (XRD)

XRD analysis is most commonly used to determine the crystallinity and physical structure of the sample after the modification. Figure 7 exhibits the XRD pattern for raw and C8 treated DPF. The diffractogram of raw and C8 treated DPF shows two peaks commonly seen in DPF [15, 29]. The first peak at 16.6°corresponding to the 101 planes represents the presence of amorphous constituents of cellulose, hemicellulose and lignin. The second peak, 23°, corresponds to the 200 planes represents the presence of α-cellulose. The experimental results reveal that during surface treatments with C8 silane, there is no structural transformation from cellulose.

Table 1 shows the crystallinity index (CI) of the raw and C8 treated DPF, calculated based on the Eq. (1). The calculated CI for the raw and C8 treated DPF was 31% and 41%, respectively. The rise in CI was observed due to the effective removal of amorphous cellulose from the fiber surface. These results are supported by the SEM micrographs, shown in Fig. 5(C-D).

Table 1
Crystallinity index of the raw and C8 treated DPF.

Type of sample	Crystallinity index (%)
Raw DPF	31
C8-DPF	41

Conclusions

In this research, DPF was able to treat with C8 silane coupling agent and modification was able to confirm through TGA, FTIR, SEM and XRD results. With treatment of C8 thermal stability increased

compared to raw DPF as per thermograms. Alkylsilane treatment effectively able to remove the non-crystalline cellulose (hemicellulose and lignin) on DPF, confirmed by TGA, SEM and XRD results. With the incorporation of silane coupling agent, hydrophilicity fiber converted into hydrophobic due to the lower surface energy by C8 silane coupling agent. The results indicated that alkylsilane-treated DPFs were a suitable reinforcing substitute for hydrophobic polymer composite.

Declarations

DATA AVAILABILITY

All data generated or analysed during this study are included in this published article. The datasets used and/or analysed during the current study available from the corresponding author on reasonable request

ACKNOWLEDGMENT

This publication was supported by grant number [113602] from Higher Colleges of Technology (HCT). Its contents are solely the responsibility of the authors and do not necessarily represent the official views of HCT.

References

1. Saheb, D. N., & Jog, J. P. (1999). Natural fiber polymer composites: a review. *Advances in Polymer Technology: Journal of the Polymer Processing Institute*, *18*(4), 351–363.
2. Bilba, K., & Arsene, M. A. (2008). Silane treatment of bagasse fiber for reinforcement of cementitious composites. *Composites part a: Applied science and manufacturing*, *39*(9), 1488–1495.
3. Zahari, W. Z. W., Badri, R. N. R. L., Ardyananta, H., Kurniawan, D., & Nor, F. M. (2015). Mechanical properties and water absorption behavior of polypropylene/ijuk fiber composite by using silane treatment. *Procedia Manufacturing*, *2*, 573–578.
4. Bilba, K., & Arsene, M. A. (2008). Silane treatment of bagasse fiber for reinforcement of cementitious composites. *Composites part a: Applied science and manufacturing*, *39*(9), 1488–1495.
5. Harish, S., Michael, D. P., Bensely, A., Lal, D. M., & Rajadurai, A. (2009). Mechanical property evaluation of natural fiber coir composite. *Materials characterization*, *60*(1), 44–49.
6. Sanjay, M. R., Siengchin, S., Parameswaranpillai, J., Jawaid, M., Pruncu, C. I., & Khan, A. (2019). A comprehensive review of techniques for natural fibers as reinforcement in composites: Preparation, processing and characterization. *Carbohydrate polymers*, *207*, 108–121.
7. Elbadry, E. A. (2014). Agro-residues: surface treatment and characterization of date palm tree fiber as composite reinforcement. *Journal of Composites*, *2014*.
8. Bezazi, A., Boumediri, H., Garcia del Pino, G., Bezzazi, B., Scarpa, F., Reis, P. N., & Dufresne, A. (2020). Alkali Treatment Effect on Physicochemical and Tensile Properties of Date Palm Rachis Fibers. *Journal of Natural Fibers*, 1–18.

9. Oushabi, A., Hassani, F. O., Abboud, Y., Sair, S., Tanane, O., & El Bouari, A. (2018). Improvement of the interface bonding between date palm fibers and polymeric matrices using alkali-silane treatments. *International Journal of Industrial Chemistry*, *9*(4), 335–343.
10. Perera, H. J., Khatiwada, B. K., Paul, A., Mortazavian, H., & Blum, F. D. (2016). Superhydrophobic surfaces with silane-treated diatomaceous earth/resin systems. Journal of Applied Polymer Science, 133(41), 44072.
11. Perera, H. J., & Blum, F. D. (2018). Alkyl chain modified diatomaceous earth superhydrophobic coatings. In *2018 Advances in Science and Engineering Technology International Conferences (ASET)* (pp. 1–4). IEEE.
12. Perera, M. H. J. (2016). Superhyrophobicity and structures of adsorbed silane coupling agents on silica and diatomaceous earth (Doctoral dissertation, Oklahoma State University).
13. Jaradat, A., & Zaid, A. (2004). Quality traits of date palm fruits in a center of origin and center of diversity. Journal of food, agriculture & environment, 2, 208–217.
14. Turner, B. (2008). Arab Organization for Agricultural Development (AOAD). In *The Statesman's Yearbook* (pp. 72–72). Palgrave Macmillan, London.
15. Oushabi, A., Sair, S., Hassani, F. O., Abboud, Y., Tanane, O., & El Bouari, A. (2017). The effect of alkali treatment on mechanical, morphological and thermal properties of date palm fibers (DPFs): Study of the interface of DPF–Polyurethane composite. South African Journal of Chemical Engineering, 23, 116–123.
16. Segal, L. G. J. M. A., Creely, J. J., Martin Jr, A. E., & Conrad, C. M. (1959). An empirical method for estimating the degree of crystallinity of native cellulose using the X-ray diffractometer. *Textile research journal*, *29*(10), 786–794.
17. Pracella, M., Chionna, D., Anguillesi, I., Kulinski, Z., & Piorkowska, E. (2006). Functionalization, compatibilization and properties of polypropylene composites with hemp fibres. Composites Science and Technology, 66(13), 2218–2230.
18. Kabir, M. M., Wang, H., Lau, K. T., Cardona, F., & Aravinthan, T. (2012). Mechanical properties of chemically-treated hemp fibre reinforced sandwich composites. Composites Part B: Engineering, 43(2), 159–169.
19. Sabarinathan, P., Rajkumar, K., Annamalai, V. E., & Vishal, K. (2020). Characterization on chemical and mechanical properties of silane treated fish tail palm fibres. *International Journal of Biological Macromolecules*, *163*, 2457–2464.
20. Han, X., Wang, L., Li, J., Zhan, X., Chen, J., & Yang, J. (2011). Tuning the hydrophobicity of ZSM-5 zeolites by surface silanization using alkyltrichlorosilane. Applied surface science, 257(22), 9525–9531.
21. Atiqah, A., Jawaid, M., Ishak, M. R., & Sapuan, S. M. (2018). Effect of alkali and silane treatments on mechanical and interfacial bonding strength of sugar palm fibers with thermoplastic polyurethane. Journal of natural fibers, 15(2), 251–261.

22. Zhou, F., Cheng, G., & Jiang, B. (2014). Effect of silane treatment on microstructure of sisal fibers. Applied Surface Science, 292, 806–812.
23. Abdelmouleh, M., Boufi, S., Belgacem, M. N., Dufresne, A., & Gandini, A. (2005). Modification of cellulose fibers with functionalized silanes: effect of the fiber treatment on the mechanical performances of cellulose–thermoset composites. Journal of applied polymer science, 98(3), 974–984.
24. Yousif, B. F., & El-Tayeb, N. S. M. (2007). The effect of oil palm fibers as reinforcement on tribological performance of polyester composite. Surface Review and Letters, 14(06), 1095–1102.
25. Chin, C. W., & Yousif, B. F. (2009). Potential of kenaf fibres as reinforcement for tribological applications. Wear, 267(9–10), 1550–1557.
26. Harper, P. W., Sun, L., & Hallett, S. R. (2012). A study on the influence of cohesive zone interface element strength parameters on mixed mode behaviour. Composites Part A: Applied Science and Manufacturing, 43(4), 722–734.
27. Zhong, J., Li, H., Yu, J., & Tan, T. (2011). Effects of natural fiber surface modification on mechanical properties of poly (lactic acid)(PLA)/sweet sorghum fiber composites. *Polymer-Plastics Technology and Engineering*, *50*(15), 1583–1589.
28. Abdelmouleh, M., Boufi, S., Belgacem, M. N., Duarte, A. P., Salah, A. B., & Gandini, A. (2004). Modification of cellulosic fibres with functionalised silanes: development of surface properties. *International Journal of Adhesion and Adhesives*, *24*(1), 43–54.
29. Liu, Y., Xie, J., Wu, N., Ma, Y., Menon, C., & Tong, J. (2019). Characterization of natural cellulose fiber from corn stalk waste subjected to different surface treatments. Cellulose, 26(8), 4707–4719.

Figures

Figure 1

(A) DPF tree (B) DPF meshes from date palm tree.

Figure 2

Fiber arrangement for on glass slide for contact angle measurement

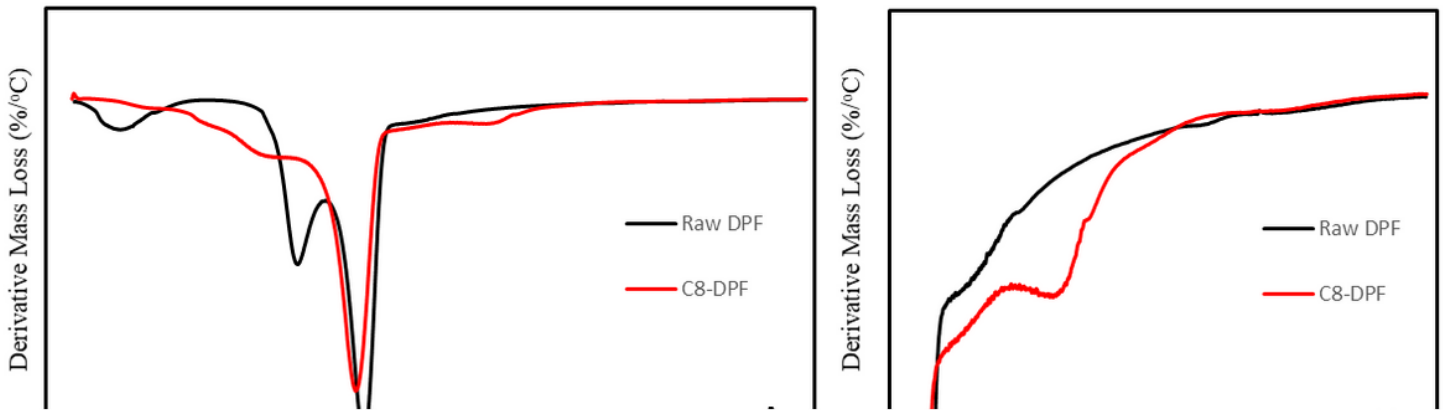

Figure 3

DTGA thermograms of raw DPF and C8-DPF.

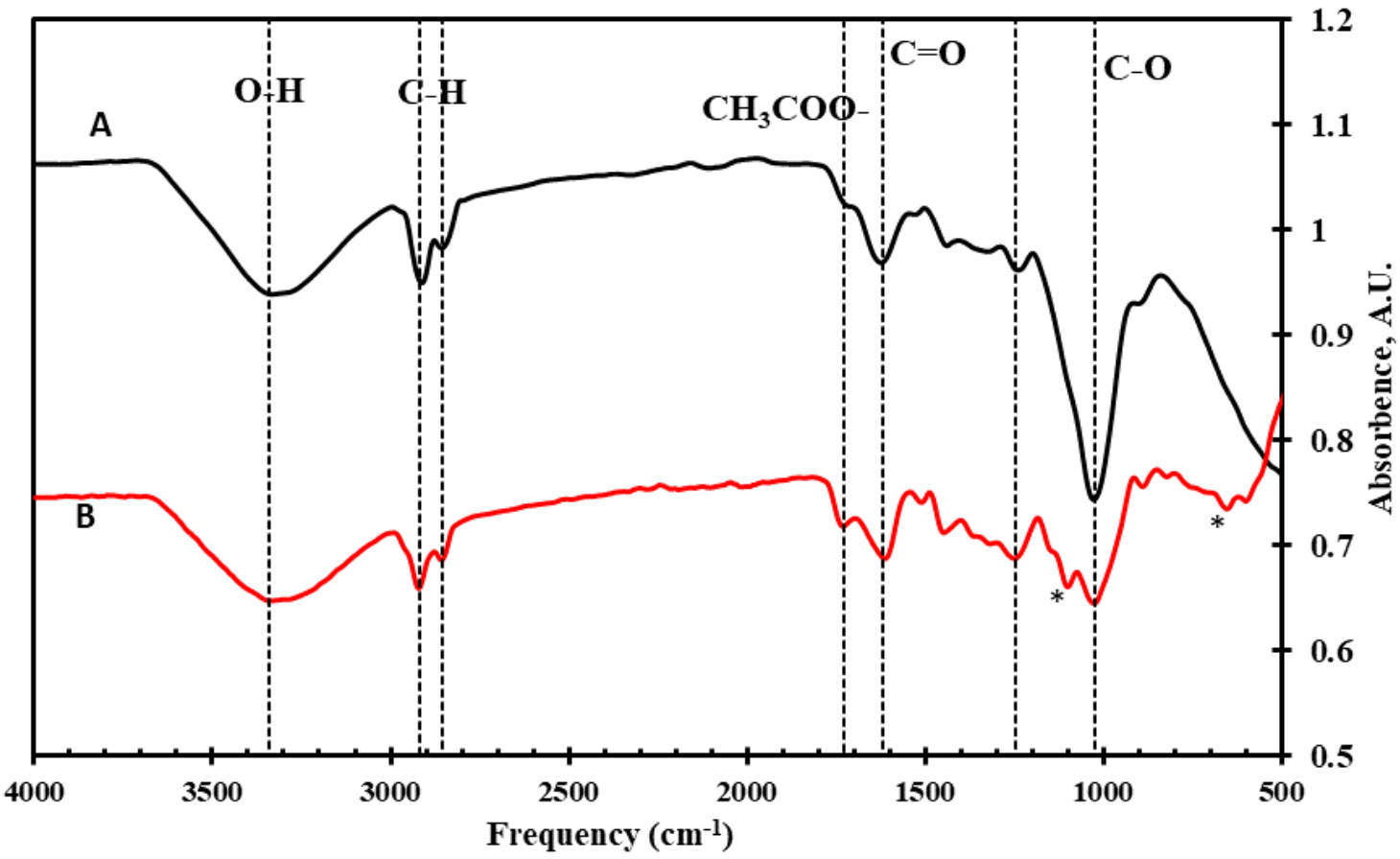

Figure 4

FTIR spectra for (A) raw DPF and (B) C8-DPF. Additional peaks appear after the C8 modification indicated with the * symbol.

Figure 5

SEM of the longitudinal surfaces of (A) raw DPF and (B) C8-DPF, the cross sections of (C) raw DPF and (D) C8-DPF.

Figure 6

The contact angles of (A) raw DPF and (B) C8-DPF.

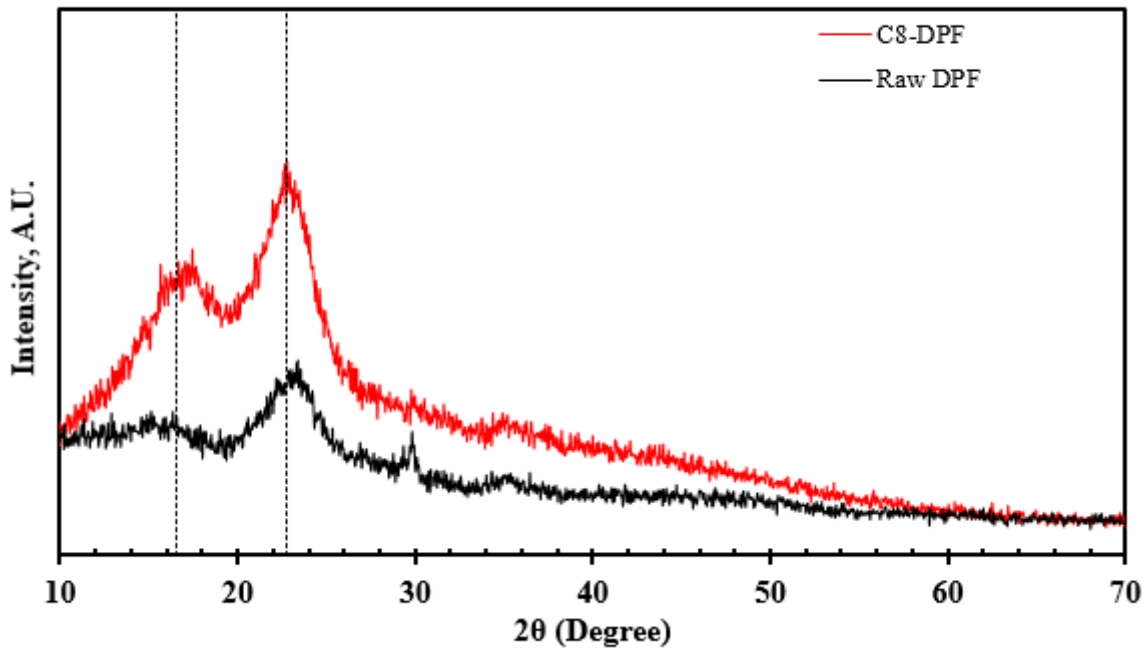

Figure 7

XRD patterns for raw and C8 treated DPF.